Dielectric Relaxation and AC Conductivity of TiO_2 Nanofiller Dispersed Polymer Nanocomposite

Anil Arya[1], Mohd Sadiq[2], A. L. Sharma[1*]

[1]Department of Physical Sciences, Central University of Punjab, Bathinda-151001, Punjab, India
[2]Department of Physics, A R S D College, Delhi -11021, India.

[a)]Corresponding author: alsharmaiitkgp@gmail.com

Abstract: The Lithium-ion conducting polymer nanocomposite (PNC) has been synthesized by the standard solution cast technique in the skeleton of PEO-PVC blend with a different content of Titanium oxide (TiO_2) as nanofiller. The lithium hexafluorophosphate ($LiPF_6$) was used as the salt. The dielectric strength decreases with frequency and is attributed to the dominance of the electrode polarization effect. The highest dielectric strength and lowest relaxation time (1.88 ns) were achieved for the 15 wt. % TiO_2 (PPS15T) PNCs when compared to other concentrations. The PPS15T exhibits the highest dc conductivity 2.34×10^{-5} S cm^{-1} at RT. The dielectric strength ($\Delta\varepsilon$) and relaxation time ($\tau_{\varepsilon'}$) were in good agreement with the dc conductivity (σ_{dc}). An interaction scheme has also been proposed to highlight the interactions between the polymer, salt and nanofiller in most visual manner.

INTRODUCTION

Now a day's development of solid polymer electrolyte has grabbed the attention of the researchers for application in batteries, fuel cells, sensors etc. Solid polymer electrolyte has advantages such as flexibility, ease of processing, electrochemical, thermal/mechanical stability over the conventional liquid electrolyte. Solid polymer electrolytes exhibit low dc conductivity while gel polymer electrolytes show desirable conductivity but have poor mechanical stability [1]. In order to improve the dc conductivity, preparation of polymer nanocomposite (PNCs) is the most feasible approach. A number of approaches are adopted, blending, cross-linking, nanofiller dispersion, nano-clay intercalation, incorporation of plasticizer. Out of the above-mentioned dispersion of nanofiller is a unique strategy to improve the conductivity [2-4]. PEO was chosen as the host polymer due to low glass transition temperature (-67 ^oC), the presence of ether group in the polymer backbone, and high dielectric constant of PEO (~ 4–5) [5]. PVC has been chosen due to the presence of a lone pair of chlorine atoms, high mechanical strength and amorphous nature [6]. The lithium hexafluorophosphate was chosen as salt due to good ionic conductivity, smaller cation size (~0.76 Å), the bulky anion (~2.8 Å) and low lattice energy [7]. The titanium oxide (TiO_2) has been chosen as nanofiller due to high dielectric constant (ε = 85) and high Lewis-acid character compared to nanofillers (such as SiO_2, ZrO_2) [8-10]. As dielectric constant is linked with the number of charge carriers, that is directly proportional to conductivity. Therefore, investigations on dielectric constant, ac conductivity and the relaxation time need to be done to understand the ion dynamics in polymeric systems [11]. In the present investigations, the TiO_2 dispersed PEO-PVC based polymer nanocomposite has been synthesized via solution cast technique. The complex permittivity, real and imaginary part of the conductivity has been investigated.

MATERIALS PREPARATION AND CHARACTERIZATION

PEO (MW= 6×10^5 g/mol), PVC (MW=6×10^4 g/mol) and $LiPF_6$ were purchased from Sigma-Aldrich. PEO, PVC, and $LiPF_6$ were dried under vacuum before use. Anhydrous tetrahydrofuran (THF) purchased from Sigma-Aldrich, was used as an aprotic solvent. All samples were prepared by the solution cast technique and detailed process is reported elsewhere [7]. The impedance measurements were performed by sandwiching the PNC film between the stainless-steel (SS) electrodes. The impedance data was further transformed into the dielectric parameters such as

DAE Solid State Physics Symposium 2018
AIP Conf. Proc. 2115, 030569-1–030569-4; https://doi.org/10.1063/1.5113408
Published by AIP Publishing. 978-0-7354-1851-6/$30.00

dielectric constant (ε'), ac impedance (σ'). All dielectric plots were fitted in the whole frequency window using Origin® 8 software to evaluate the dielectric strength, dc conductivity and relaxation time. The complex dielectric permittivity is expressed as by equation 1 [12]:

$$\varepsilon^* = \varepsilon' - j\varepsilon'' ; \ \varepsilon' = \epsilon_\infty + \frac{\Delta\varepsilon\left(1+x^\alpha \cos\frac{\alpha\pi}{2}\right)}{1+2x^\alpha \cos\frac{\alpha\pi}{2}+x^{2\alpha}} \quad (1)$$

Where, where ε' the real part of the complex permittivity is, α is distribution parameter and $x = \omega\tau$; ω is angular frequency of applied field and τ is average Debye relaxation time. The real and imaginary part of the conductivity is expressed as equation (2) [13].

$$\sigma' = \frac{\sigma_b^2 C_{dl}\omega^\alpha \cos\left(\frac{\alpha\pi}{2}\right) + \sigma_b (C_{dl}\omega^\alpha)^2}{\sigma_b^2 + 2\sigma_b C_{dl}\omega^\alpha \cos\left(\frac{\alpha\pi}{2}\right) + (C_{dl}\omega^\alpha)^2} , \sigma'' = \frac{\sigma_b^2 C_{dl}\omega^\alpha \sin\left(\frac{\alpha\pi}{2}\right)}{\sigma_b^2 + 2\sigma_b C_{dl}\omega^\alpha \cos\left(\frac{\alpha\pi}{2}\right) + (C_{dl}\omega^\alpha)^2} + \omega C_b \quad (2)$$

Where, C_{dl} is frequency independent double layer capacitance, ω is the angular frequency, s & α are exponent terms with value <1 and C_b is the bulk capacitance of solid polymer electrolyte.

RESULT AND DISCUSSIONS

DIELECTRIC PERMITTIVITY ANALYSIS

The role of nanofiller in enhancing the dielectric constant is investigated by plotting the real part of complex permittivity. The real part of the complex permittivity i.e. dielectric constant indicates the polarizing ability of electrolyte on the application of field [14-15]. Figure 1 a, depicts the real part of dielectric permittivity and dielectric constant decreases with frequency for all systems. It is interesting to note that the addition of nanofiller increase the dielectric constant as compared to the polymer salt system and is attributed to the electrode polarization owing to the ion accumulation at blocking electrodes. It hinders the long-range ion migration.

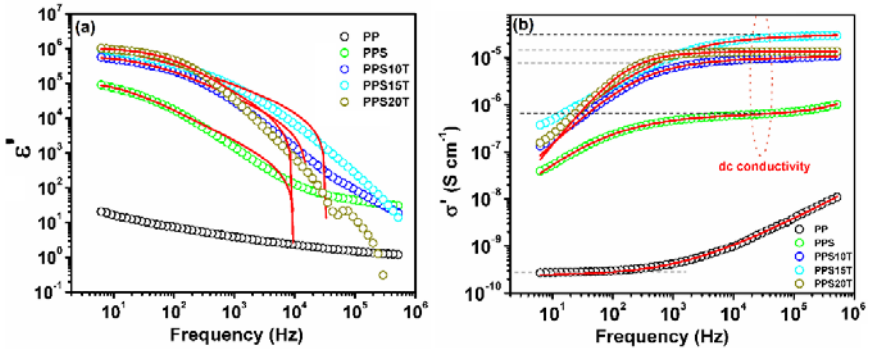

FIGURE 1. (a) Plot of dielectric constant, and (b) ac conductivity against the frequency for solid polymer electrolytes.

TABLE 1. The fitted ε' (ε_∞, $\Delta\varepsilon$, $\tau_{\varepsilon'}$, α) parameters at room temperature.

Sample Code	ε_∞	$\Delta\varepsilon(\times 10^6)$	$\tau_{\varepsilon'}$(ns)	α
PP	10	0.01	327	0.625
PPS	492	0.12	25	0.724
PPS10T	6906	0.65	5.74	0.658
PPS15T	14559	1.35	1.83	0.558
PPS20T	9714	1.04	5.31	0.772

The decrease of dielectric constant in the high-frequency window is due to the presence of dielectric relaxation [16]. Table 1 shows the fitted parameters and the solid red line is fitted plot. It may be noticed that the dielectric strength ($\Delta\varepsilon = \varepsilon_s - \varepsilon_\infty$) increases with the addition of nanofiller and relaxation time decreases. The reduction of the relaxation time indicates the faster polymer chain segmental motion [17].

REAL PART OF COMPLEX CONDUCTIVITY

The complex conductivity (σ^*) is expressed as, $\sigma^* = \sigma' + i\sigma''$, where σ' is the real part of conductivity, σ'' is the imaginary part of conductivity. Figure 1 b shows the plot of real part of the complex conductivity against the

frequency. The plot comprise of three regions, (i) low frequency electrode polarization region due to electrode polarization effect, (ii) intermediate frequency region indicates long-range ion dynamics, and (iii) high frequency dispersion region indicates hopping process and is associated with ac conductivity. The dc conductivity is extracted from the intercept on the intermediate region (shown by dotted line) [18]. The solid red line shows the fitted plot in the whole frequency window and is in perfect agreement with the experimental data. Table 1 shows the fitting parameters and it may be noted that dc conductivity is highest for the 15 % TiO_2 system. The increase in the dc conductivity is due to two reasons, (i) enhanced amorphous content, and (ii) enhanced polymer chia segmental motion.

TABLE 2. Comparison of fitted parameters for real and imaginary part of complex conductivity.

Sample Code	σ'				σ''				
	σ_b (S cm^{-1})	α	n	C_{dl} (μF)	A (S cm^{-1})	s	C_{dl} (μF)	α	C_b(pF)
PP	4.12×10^{-9}	0.856	0.534	1.14	1.32×10^{-9}	0.28	0.001	0.95	0.89
PPS	6.35×10^{-7}	0.752	0.632	7.81	2.29×10^{-8}	0.08	0.012	0.96	2.68
PPS10T	9.23×10^{-6}	0.470	0.531	30.14	3.12×10^{-5}	0.37	0.082	0.77	13.8
PPS15T	2.34×10^{-5}	0.125	0.725	90.02	5.08×10^{-4}	0.41	0.304	0.57	15.9
PPS20T	6.71×10^{-6}	0.347	0.652	23.01	2.07×10^{-5}	0.60	0.057	0.99	3.37

IMAGINARY PART OF COMPLEX CONDUCTIVITY

Figure 2 shows the frequency dependent imaginary part of the complex conductivity and the solid red line is the fitted plot. It may be noted that both experimental and fitted data are in good agreement and fitted parameters are summarized in Table 2. The plot displays two frequency, (i) maximum frequency (ω_{max}) associated with maximum polarization, and (ii) onset frequency (ω_{on}) associated with initialization of polarization built-up [19-20]. All polymer system shows a minima in the σ'', and at this frequency real part of complex conductivity (σ'; Figure 1 b) shows dispersion region. In the plot, with decrease of frequency σ'' decreases upto ω_{on} followed by increase with a maxima which corresponds to the dispersive region in the plot of real part of conductivity with the frequencyω_{max}. Figure 2 b shows the increase of ω_{max} with addition of nanofiller (maxima for 15 % the TiO2) and confirms the increases polarization window owing to increase of number of charge carriers.

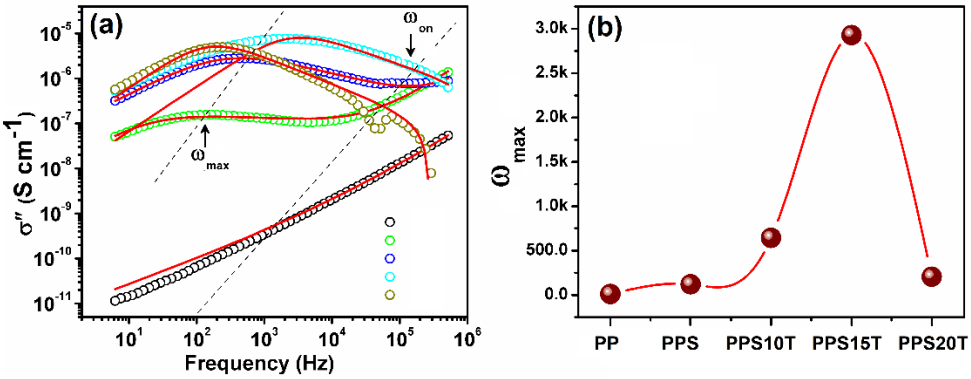

FIGURE 2: (a) plot of imaginary part of complex conductivity against the frequency, and (b) Variation of ω_{max} for different nanofiller content.

CORRELATION OF DIELECTRIC STRENGTH, RELAXATION TIME & DC CONDUCTIVITY

Figure 3 a shows the variation of the dielectric strength ($\Delta\varepsilon$), relaxation time ($\tau_{\varepsilon'}$)& dc conductivity (σ_{dc}) for different polymeric systems. The dielectric strength increases with the addition of nanofiller in the polymer salt matrix and indicates the better salt dissociation or increased dielectric constant ($\Delta\varepsilon = \varepsilon_s - \varepsilon_\infty$). The maxima was obtained for the 15 % TiO_2 system (PPS15T). The relaxation time decreases with the addition of the nanofiller and indicates the faster ion migration via the coordinating sites provided by the electron rich ether group of PEO. The lowering of the relaxation time provides direct evidence of increased dc conductivity.

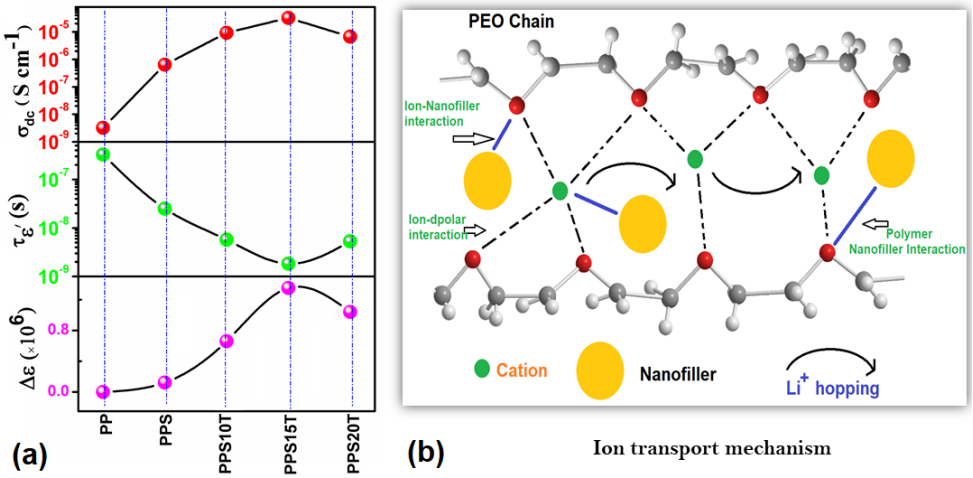

FIGURE 3: (a) plot of the variation of dielectric strength ($\Delta\varepsilon$), relaxation time ($\tau_{\varepsilon'}$)& dc conductivity (σ_{dc}) for different solid polymer electrolyte, and (b) ion transport mechanism in nanofiller dispersed polymer nanocomposite.

It is interesting to note that the dc conductivity plot shows the maxima for the 15 % TiO_2 system. It may be concluded that a good correlation is obtained between all the three parameters and confirms the suitability of the present system for energy storage devices. Figure 3 b shows the ion transport mechanism in the nanofiller dispersed polymer nanocomposites. It indicates the modification of the interactions between the polymer-ion and leads to ease of ion migration. Addition of nanofiller further alters the interactions and main interactions are, (i) polymer-nanofiller interaction that reduces the chain reorganization tendency of polymer chains, (ii) cation-polymer interaction due to cation coordination for hopping, and (iii) cation-nanofiller interaction, here surface group (-OH) of nanofiller provides additional coordinating sites for cation migration. It may be summarized the nanofiller plays an effective role in enhancing the ion transport and is evidenced by the high dc conductivity, high dielectric strength and low relaxation time.

ACKNOWLEDGMENTS

One of the authors (AA) is thankful to the Central University of Punjab, Bathinda for providing fellowship.

REFERENCES

1. A. Arya, A. L. Sharma, Ionics, **23**, 497-540 (2017).
2. L. Long, S. Wang, M. Xiao, Y. Meng, Journal of Materials Chemistry A, **4**, 10038-10069 (2016).
3. A. Arya, A. L. Sharma, Journal of Solid State Electrochemistry, **1-21** (2018).
4. Y. Kim, S. J. Kwon, B. M. Jung, S. B. Lee, U. H. Choi, Chem of Materials, **29**, 4401-4410 (2017).
5. A. Arya, A. L. Sharma, Journal of Physics D: Applied Physics, **50**, 443002 (2017).
6. R. Arunkumar, R. S. Babu, M. U. Rani, J Mate Science: Materials in Electronics, **28**, 3309-3316 (2017).
7. A. Arya, A. L. Sharma, Journal of Physics D: Applied Physics, **51**, 045504 (2018).
8. S. R. Mohapatra, A. K. Thakur, R. N. P. Choudhary, J. Polym. Sci. B **47**, 60 (2008).
9. S. H. Chung, Y. Wang, L. Persi, F. Croce, , B. Scrosati, E. Plichta J. Power Sources **97**, 644 (2011).
10. A. Arya, M. Sadiq, A. L. Sharma, Ionics, **24**, 2295-2319 (2018).
11. P. S. Anantha, K. Hariharan, Mater Sci Eng B Solid-State Mater Adv Technol **121**, 12–19 (2005).
12. W. Cao, R. Gerhardt, Solid State Ionics **42**, 213-221(1990).
13. A. Roy, B. Dutta, S. Bhattacharya, RSC Advances **6**, 65434-65442 (2016).
14. K. S. Cole, J. Chem. Phys. **9**, 341-351 (1940).
15. A. Arya, S. Sharma, A. L. Sharma, D. Kumar, M. Sadiq, Asian J Eng Appl Technol **5**, 4-7 (2016).
16. N. Chilaka, S. Ghosh, Electrochimica Acta **134**, 232-241 (2014).
17. A. Arya and A. L. Sharma, Journal of Physics: Condensed Matter **30**, 165402 (2018).
18. S. Choudhary and R. J. Sengwa, Materials Chemistry and Physics. **142**, 172-181 (2013).
19. Y. Wang, C. N. Sun, F. Fan, M. B. Berman,... and A. P. Sokolov, Physical Review E **87**, 042308 (2013).
20. S. Das and A. Ghosh, The Journal of Physical Chemistry B **121**, 5422−5432 (2017).